Agricultural Water Management 302 (2024) 108988

Contents lists available at ScienceDirect

Agricultural Water Management

journal homepage: www.elsevier.com/locate/agwat

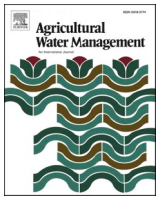

Mapping of irrigated vineyard areas through the use of machine learning techniques and remote sensing

Esther López-Pérez [a,*], Carles Sanchis-Ibor [b,c], Miguel Ángel Jiménez-Bello [a], Manuel Pulido-Velazquez [a]

[a] Research Institute of Water and Environmental Engineering (IIAMA), Universitat Politècnica de València, Camí de Vera s/n, València 46022, Spain
[b] Valencian Center for Irrigation Studies (CVER), Universitat Politècnica de València, Camí de Vera s/n, València 46022, Spain
[c] Department of Geography, Universitat de València, Av.Blasco Ibáñez 28, València 46010, Spain

ARTICLE INFO

Handling Editor: J. E. Fernández

Keywords:
Irrigated area
Machine Learning
Remote sensing
Soil moisture

ABSTRACT

Effective and sustainable management of aquifers in regions with intensive groundwater use for irrigation requirements accurate mapping or irrigated areas to control water resource exploitation and plan rational water usage. This study proposes a cost-effective methodology based on satellite images to identify irrigated areas utilizing surface water and groundwater resources. The methodology integrates soil moisture estimations, environmental variables, and variables that affect to retention of water soil, that join a ground truth dataset, to estimate irrigated surface through a machine learning method during the irrigation period of 2021. Spectral data derived parameters and crop morphology, along with official data on agricultural parcels, were utilized to define vineyard irrigation areas at the plot scale within the Requena-Utiel aquifer in Eastern Spain. A machine learning classification technique was applied,yielding a remarkable precision of 91.8 % when compared to ground truth data.Discrepancies between the remote sensing-based irrigated area estimation and official data are highlighted. This study represents the most accurate plot-scale irrigation mapping of woody crops in the region to date.

1. Introduction

Groundwater has been the main driver of the "silent revolution" that has enabled the expansion of irrigation in many regions of the globe (Giordano, 2009; Llamas and Martínez-Santos, 2005; Molle et al., 2018; Shah et al., 2007). In many cases, this revolution has led to severe over-exploitation of aquifers, with negative consequences for the viability and profitability of agriculture, for the future of food production, and for the sustainability of aquatic ecosystems (Gleeson et al., 2012; Grogan et al., 2017). These problems arise from the lack of interest and/or means of the authorities to control the expansion of groundwater irrigation. On numerous occasions, the hydraulic administrators/bureaucracies have promoted these policies to boost agricultural revenue. However, when the public sector begins witnessing inefficiencies, they struggle to find effective mechanisms to regulate excessive water withdrawals (Molle and Closas, 2020a, 2020b). The "silent" almost anonymous nature of groundwater exploitation has posed a challenge for the management and governance of many aquifers due to the difficulty in avoiding the free-rider behavior of many users, some of whom have powerful vested interests (Hoogesteger and Wester, 2018, 2015). The "silence" of the revolution is synonymous with opacity and, therefore, a source of frequent inequalities (Ameur et al., 2017; Damonte and Boelens, 2019).

Experts have proposed various approaches to address this problem, some based on improved governance, others on coercive control and sanction measures, and increasingly on mixed "sticks" and "carrots" policies (Birkenholtz, 2015; Closas et al., 2017; López-Gunn, 2012; Molle et al., 2018; Molle and Closas, 2020). In almost all cases, having tools to estimate the irrigated area is essential. Sustainable groundwater management relies on data (Sharples et al., 2020). Without a clear knowledge of the use and users of the common resource, it is significantly more challenging to develop state-led policies or the preferable collective management instruments that allow sustainable exploitation (Rouillard et al., 2021; Petit et al., 2021).

It is, therefore, necessary to measure the degree of exploitation of groundwater resources in an efficient and quantifiable way. To this end, geospatial analysis methodologies using remote sensing techniques and geographic information systems have been identified as having great

* Corresponding author.
E-mail address: estloppe@upv.es (E. López-Pérez).

https://doi.org/10.1016/j.agwat.2024.108988
Received 23 October 2023; Received in revised form 28 May 2024; Accepted 2 August 2024
Available online 20 August 2024

potential for sustainable environmental management (Bouasria et al., 2021b; Bounif et al., 2021; Rahimi et al., 2021). The rapid advancement in remote sensing technologies has enabled their application as a crucial and emerging data source for environmental dynamics and agricultural changes in recent years (Bouasria et al., 2021a; Mjiri et al., 2022; Rahimi et al., 2022). In this context, the identification of irrigated areas proves highly beneficial and has demonstrated relative success when applied in diverse regions of the world (Ambika et al., 2016; Brown and Pervez, 2014; Castaño et al., 2010; Foster et al., 2020; Vogels et al., 2019; Xie et al., 2021).

The use of satellite imagery allows the development of digital thematic maps describing the spatial distribution of the irrigated land. These technologies use mathematical algorithms that describe the connection between the signal captured by the sensor and the surface water content. Given a sequence of multi-spectral and multi-temporal images, a classification process assigns an irrigation label to each pixel. Some methods use Vegetation Indices from optical data for long periods to understand interannual variability in irrigated areas (Ambika et al., 2016). Following vegetation indices, it is proposed to monitor seasonal irrigated cropland for quantifying areas under groundwater irrigation using multiple optical satellite images to fill data gaps during crop growth periods due to clouds in tropical regions (Sharma et al., 2021), others compile relevant vegetation indices and climate variables for mapping and quantifying irrigated and dry land agriculture areas (Zurqani et al., 2021).

Other satellites use global soil moisture (SM) data to classify irrigated areas (Bazzi et al., 2019; Gao et al., 2017; Pageot et al., 2020; Rabiei et al., 2021; Zohaib et al., 2019). These satellites such as SMOS and SMAP use microwave radiometers, specifically L-band, to measure SM in the first 10 cm of the soil profile. The method is based on the large contrast of the dielectric properties of water and soil properties and showed promise for monitoring soil moisture in agricultural areas (Wigneron et al., 1996, 2017). However, the measurements obtained by the radiometers are limited to within a few centimeters of the surface, and they are unable to directly capture the soil moisture conditions of the roots. In addition, these satellite data have a low spatial resolution (35–50 km), although methods based on downscaling microwave products through optical data have recently been developed (Dari et al., 2021).

Several studies have demonstrated the effectiveness of combining optical and synthetic aperture radar (SAR) time series data for accurate SM estimation in crops with dense vegetation cover, such as cereals (Bazzi et al., 2019; Gao et al., 2018). The use of this data to monitor SM is significant as it is not affected by cloud cover and provides a high temporal resolution. However, for other types of crops, such as woody crops with high ground surface dominance, SAR data have a dominant direct return from the ground surface and a multiple scattering component that results in disturbing and unmodelled signal fluctuations of soil and low-cover vegetation (Ballester-Berman et al., 2013).

Recently, a promising optical method, called Optical TRApezoid Model (OPTRAM) has emerged as an effective approach for calculating SM. The method is based on the Thermal-Optical TRApezoid Model (TOTRAM), also known as the “trapezoid” or “triangle” model, which measures SM using the Normalized Difference Vegetation Index (NDVI) of optical and thermal data (Sadeghi et al., 2015). Unlike the “triangle” model, the OPTRAM method uses a physical relationship between NDVI and shortwave infrared reflectance (SWIR), parameterized in an index called shortwave infrared transformed reflectance (STR). This method has some advantages over TOTRAM as it can estimate soil moisture directly from sensor observations that lack a thermal band, in addition, thermal bands have a coarser spatial resolution compared to visible, near-infrared, and mid-infrared bands. This enables the use of a greater range of satellites, such as Sentinel 2, improving spatial and temporal resolution without the need to use thermal data. The OPTRAM method has been applied in recent studies to determine the soil moisture content at the watershed scale (Mananze and Pôças, 2019; Sadeghi et al., 2017a) and at the plot scale (Babaeian et al., 2019, 2018; Chen et al., 2020).

The promising results of OPTRAM have allowed us to develop a methodology consisting of image classification in machine learning classifiers that are used as decision trees (Brodley and Friedl, 1997). In recent years, the Random Forest (RF) method, applied to geographical objects, has gained increasing attention in the literature. It has proven to be an effective approach for analyzing high spatial resolution imagery (Blaschke, 2010) and has shown promising results in crop mapping using remotely sensed data in recent years (Akbari et al., 2020; Devkota et al., 2024; Htitiou et al., 2019).

The expansion of groundwater irrigation in semi-arid regions of Spain threatens its sustainability (De Stefano et al., 2014, 2015). Consequently, water authorities and certain irrigation users have been actively seeking efficient methods to restrict irrigation expansion and manage groundwater overexploitation (Calera et al., 2017). Mapping irrigated areas provides important data to improve the control and management of groundwater use. The study’s main objective is to develop an inexpensive and efficient method to detect irrigated areas of woody crops at the plot scale. The method employs remote sensing and geographical data classification, along with artificial intelligence techniques to provide insights into the decision-making process of individual irrigators. This promotestransparent collective groundwater management.

2. Study area

The Requena-Utiel aquifer is located in the interior of the Valencian Community and spans most of the Requena-Utiel region (Fig. 1). Vineyards cover 304.2 km2, which represents 90 % of the agricultural land. The map uses different colours to distinguish between rain-fed and irrigated vineyards. It also indicates vineyards that have consolidated water rights in 2018, as indicated by the Jucar River Basin Authority. Specifically, green colour specifically represents vineyards with consolidated water rights, while clear orange is used for both rain-fed vineyards. The groundwater system covers an area of 987.9 km2 with an altitude ranging from 600 to 1200 m above sea level. The average slope is 5 %.

The area has a Mediterranean climate with some continental influence, falling between the Köppen-Geiger Csa and Csb types. The mean annual temperature is 14°C and a mean annual rainfall is 323 mm. The irrigation season aligns with the driest part of the year, from June to August (Fig. 2). The majority of soils have a clayey texture, except for a narrow alluvial ridge along the Magro River.

In 1995, according to the statistics of the regional administration (GVA, 2021), the irrigated area of Requena-Utiel occupied 1738 ha, of which 1279 ha were forage and summer vegetables, and 449 ha dedicated to wine vineyards. The rest of the region was occupied by rainfed crops (58,524 ha), with 44,445 ha being vineyards. However, by 2019, the irrigated area had significantly expanded to 11,660 ha of vineyards, 1546 ha of almond trees and 1415 ha of secondary crops. Since 1995, the irrigated area had increased eight-fold. In most instances, the development of new irrigation land has been made possible by installing drip irrigation systems and vine trellises, driven by several factors. In the absence of river resources, farmers promoted this transformation by drilling wells. Irrigated crops expanded due to: i) the search for increased production; ii) the promotion of irrigation modernization through subsidies by the regional government; and iii) the evidence of global warming and the trend of decreasing rainfall. However, this process was conducted without proper planning or assessment of water resources, jeopardizing the sustainability of the groundwater system.

In 2016, the Jucar River Basin Authority approved the *Exploitation plan of the Requena-Utiel groundwater body*. This plan, established a water allocation of 450 m^3/ha for woody crops and wet years (900 m^3/ha for dry years, and 600 m^3/ha for average years) to users with administrative concessions. As part of this plan, irrigation was not allowed for those areas that do not have administrative water concession until 2016 (CHJ,

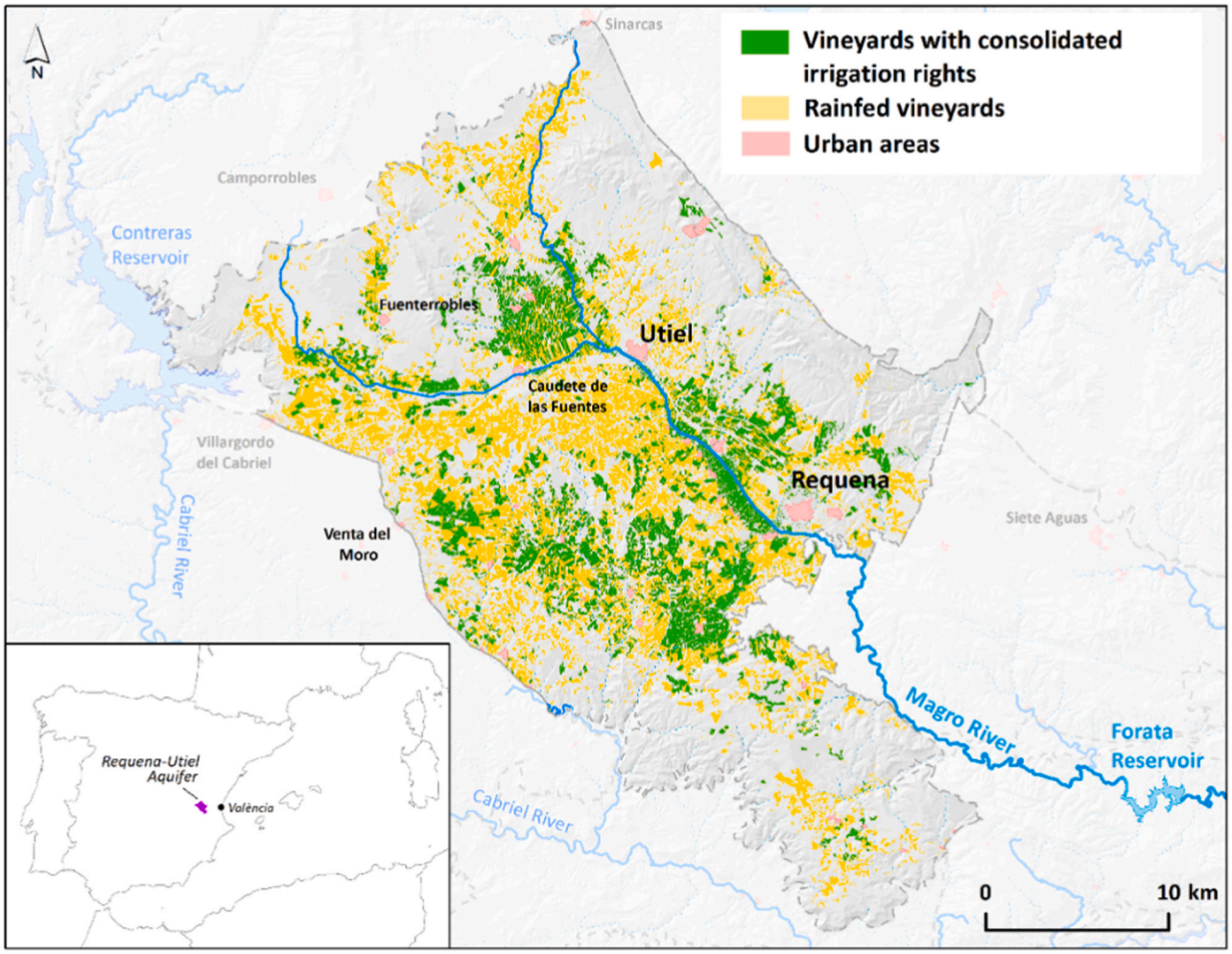

Fig. 1. Consolidated water rights mapping of the Requena-Utiel aquifer (source: CHJ, 2019).

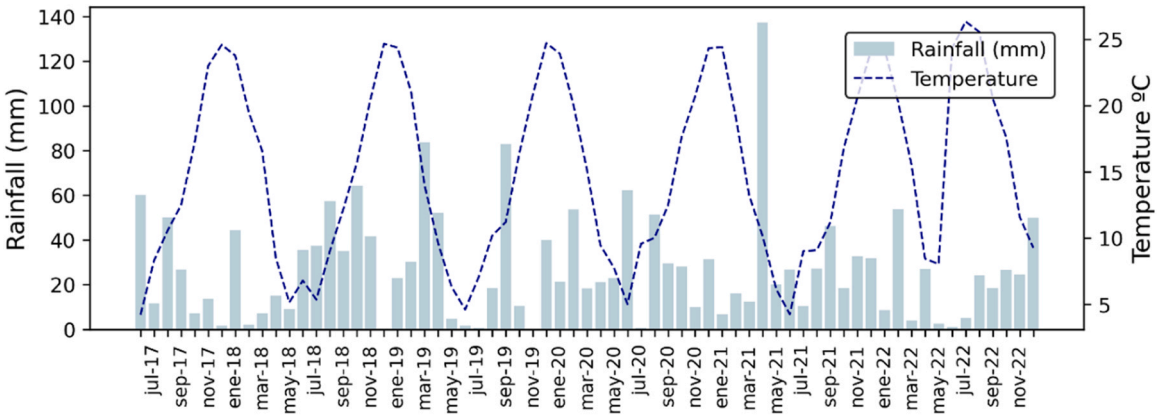

Fig. 2. Temporal behavior of ambient temperature and precipitation for the last five years 2017–2023. Source: SIAR (acronym for Agroclimatic Information System for Irrigation).

2016). This plan has subsequently been updated without significant changes (CHJ, 2020).

The existing official data regarding the irrigated area are highly inconsistent, as shown in Table 1. The Jucar River Basin Authority estimates an area with consolidated water rights of 16,220 ha (inclouding 12,852 ha of vineyards), and the regional government estimates 13,844 ha of irrigated land (of which 11,771 ha are vineyards) (CHJ, 2019; GVA, 2021). This discrepancy arises because the Jucar River Basin

Table 1
Irrigated from official data (ha) in study area.

	River Basin Authority	Regional Government
Total irrigated area	16,220	14,621
Irrigated vineyard area	12,852	11,660

Authority registers land with water rights, while the Regional Government estimates irrigated land based on a survey, often resulting in underestimations of the actual irrigated lands. Due to legal requirements, farmers have had to join other users in an institution for the collective management of the aquifer. However, they do not have precise knowledge of the actual extent of the irrigated area. Additionally, in the Requena-Utiel district, the non-irrigated area spans from 41,542 ha to 45,785 ha, out of which 23,139 ha to 24,185 ha consist of vineyards, (GVA, 2021; SIGPAC, 2021). Both individual farmers and collective organizations are seeking the expansion of non-irrigated areas to irrigated ones (Sanchis-Ibor et al., 2023). The further development of reliable tools for estimating irrigated land is crucial.

3. Material and methods

This study uses spatial information and artificial intelligence techniques to estimate the groundwater irrigated area of Requena-Utiel at the plot scale. Random Forest was used as a classifier on crop plots, configured as vector spatial objects to predict the irrigated area. The value of the crop plot was determined by averaging the pixels that fall within them, thus reducing intra-plot variability and excluding anomalous pixels. The analysis combines geographical data influencing crop water status with soil moisture information and climate data from multispectral imagery during the 2021 irrigation period.

The boundaries of the groundwater system were determined based on the official mapping of groundwater bodies (CHJ, 2021). The land use layers consist of both graphical and alphanumeric data, providing the geographical reference of each plot, surface and land use data, and other relevant details (SIGPAC, 2021). That is the geographical reference of each data plot on surface and land use and relevant details. Basic information on vineyard characteristics was provided by the Designation of Origin's Regulatory Council (CRDO). Geomorphological data, acquired from the Territorial Action Plan on the Flood Risk Prevention in the Region of Valencia, PATRICOVA (2021), along with topographic information such as slope and aspect, were provided by ALOS World 3D (AW3D30) dataset. These datasets were integrated into Geographic Information Systems as input data.

Sentinel-2 multispectral data from the Copernicus programme (Earth Observation component of the European Union's space programme) were used to estimate soil moisture by combining spectral bands with the OPTRAM method. To eliminate the potential influence of rainfall on the soil moisture conditions of the plot, CHIRPS satellite images were used for spatial mapping of rainfall. We opted for Google Earth Engine (GEE) as our analytical platform for acquiring spectral bands. GEE makes it possible for sequences of images to be loaded and resampled. GEE employs an image pyramid based on the closest scale that is less than or equal to the average of the pixels in the immediate lower level. The analysis scale was determined based on the 10 m output to have the highest possible resolution and based on the resolution of the Sentinel 2 multispectral used in the model.

Topographic and multispectral data and soil moisture estimates were combined with the land use map using algebraic mapping techniques, and mean plot values were obtained for all variables. In addition, both irrigated and rainfed plots were used as reference data to train the machine learning classifier. Finally, RF was applied as a classification technique on a vector database to estimate the irrigated area. Fig. 3 shows the workflow and sequence of operations performed.

3.1. OPTRAM model implementation

The OPTRAM model is based on the linear physical relationship between soil moisture and STR (2). The model is parameterized as a function of the spatial distribution of the pixel between a vegetation index and the STR. The method aims to replace the land surface temperature (LST) of its predecessor method, the Thermal Optical Time-series Ratio-based Algorithm (TOTRAM) with a humidity measure-

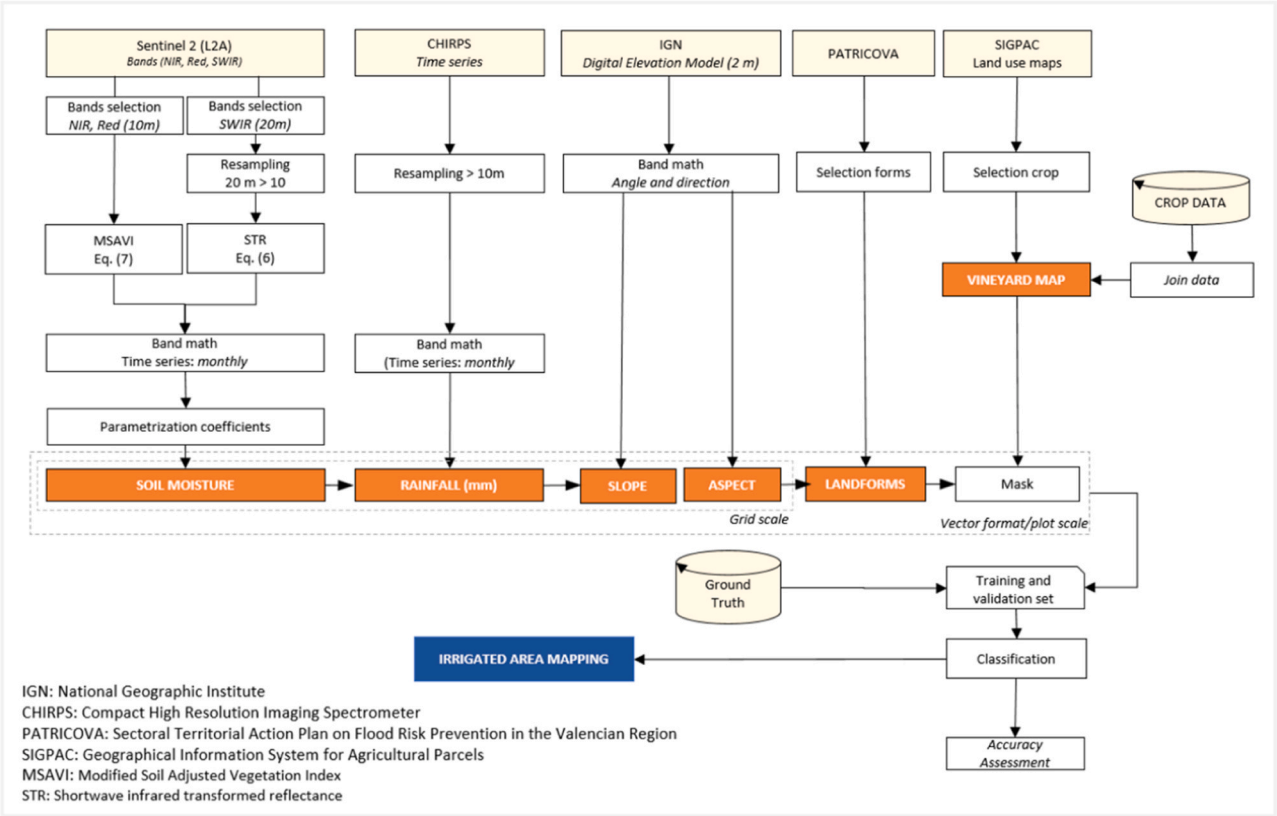

Fig. 3. Flowchart representing the workflow overview.

ment in the optical domain. Thus, the method develops a linear physical relationship between soil moisture (W) (1) and shortwave infrared reflectance (SWIR). The model has been shown to have high accuracy in the 2210 nm region of the electromagnetic spectrum (Sadeghi et al., 2017a, 2015).

$$W = \frac{\theta - \theta_d}{\theta_w - \theta_d} = \frac{SRT - STR_d}{STR_w - STR_d} \quad (1)$$

STR is related to the SWIR band as follows:

$$STR = \frac{(1 - R_{SWIR})^2}{2 * R_{SWIR}} \quad (2)$$

Where STRd and STRw are STR at dry (e.g., θ ~0 cm^3 cm^{-3}, where θ is volumetric moisture content) and wet (e.g., θ=θs cm^3 cm^{-3}, where θs is saturated moisture content) states, respectively (Babaeian et al., 2018). R_{SWIR} is the reflectance in the short-wave infrared.

Recent research has shown that normalized vegetation indices represent the variability of vine vegetation, which, in turn, is related to soil water stress. In other words, soil moisture influences the water status of the crop, and this is reflected in the spectral characteristics of the vegetation. Therefore, the OPTRAM method proposes the Normalized Difference Vegetation Index (NDVI) to estimate soil moisture. To use OPTRAM for woody crops, we replaced the NDVI vegetation index with the Modified Soil Adjusted Vegetation Index (MSAVI2) (3) (Qi and Kerr, 1994; Qi et al., 1994; Richardson and Wiegand, 1977).

The MSAVI2 index utilizes the red band (RED) to detect the strong absorption of chlorophyll, resulting in increased values when vegetation cover is sparse. Additionally, the near-infrared band (NIR) is used, and its reflection by the vegetation is reduced to enhance the sensitivity of the index to the combined effects of vegetation and soil (Xue and Su, 2017). Recent research (Babaeian et al., 2019; Towers et al., 2019) has demonstrated that the MSAVI2 is more sensitive to vegetation in areas where soil plays a significant role in land cover.

$$MSAVI2 = 0.5 * [(2\mathrm{NIR} + 1) - \sqrt{(2NIR + 1)^2 - 8(NIR - Red)}] \quad (3)$$

Assuming an empirical linear relationship of STRd and STRw with the vegetation fraction, the dry and wet edges of the optical trapezoid are defined as follows (see Fig. 4, which illustrates the relationship between STRd, STRw, and the vegetation fraction).

Therefore, STR answers to the linear relationship at the wet and dry boundary as follows:

$$STR_d = i_d + s_d MSAVI2 \quad (3)$$

$$STR_w = i_w + s_w MSAVI2 \quad (4)$$

Where $i_d$ands_d are the limit and the slope of the dry point, and i_w, s_w are the limit and the slope of the wet point.

By combining the equations, the soil moisture at each pixel can be estimated as a function of STR and MSAVI2:

$$W = \frac{i_d + s_d MSAVI2 - STR}{i_d - i_w + (s_d - s_w)MSAVI2} \quad (5)$$

The spacing between STR-MSAVI2 is expected to be invariant since reflectance is a function that only considers soil properties and not atmospheric conditions. Thus, a universal relationship applicable to all dates at a specific site is anticipated (Babaeian et al., 2018; Sadeghi et al., 2017a).

The multispectral data required to implement the OPTRAM model were acquired from the Sentinel-2 (S2) satellite. The selected bands (Near Infrared band, NIR (b8): Shortwave, InfraRed band, SWIR (b12); and Red band, RED (b4)), already corrected, were selected without cloud cover (Sentinel-2 L2A). The S2 data have a high spatial resolution (10–20 m) and a temporal imaging frequency of 5 days. During the 3-month dry season, a total of 54 scenes were used and analyzed using 3 spectral bands: Short-Wavelength Infrared (SWIR), Near-Infrared (NIR), and Red (RED). These spectral bands were employed to monitor soil moisture levels throughout the dry season and predict whether the parcel was irrigated. The data collected from the scenes provided valuable insights into how soil moisture varied over time.

3.2. Climate dataset

Rainfall data were obtained from the Climate Hazards Group Infra-Red Precipitation with Station data (CHIRPS) provided by the United States Geological Survey (USGS) and the University of California, Santa Barbara (UCSB). CHIRPS is a valuable resource used in areas with limited weather stations. It incorporates a monthly rainfall dataset of 0.05° resolution satellite imagery and in-situ station data (Funk et al., 2015).

CHIRPS data provide an image showing total rainfall every five days. A total of 18 images taken during the three-month irrigation period (or dry season) were used as input data. These images were summarized by adding the rainfall amounts to create three monthly images. The original CHIRPS data resolution was resampled to achieve a 10 meter spatial resolution to align with output resolution in Google Earth Engine (GEE).

3.3. Characteristics of terrain surface and landforms

Certain factors, such as landforms and relief characteristics, influence moisture retention and aid in distinguishing between naturally wet plots (e.g., shaded areas or valleys) and plots that receive irrigation water. The physical characteristics of land, including slope and aspect, play a crucial role in this process. Slope and aspect determine the amount of solar radiation the soil receives, directly affecting soil moisture conservation. For this study, a global digital surface model (DSM) with a resolution of 30 m, provided by the ALOS World 3D (AW3D30) dataset, was used as input data. The slope and aspect of each plot were obtained from AW3D30 and resampled to a 10 m spatial resolution using GEE.

The aquifer is situated in a plain characterized by flat terrain and covered by an extensive pediment, intersected by the narrow floodplain of the Magro River. These geomorphological units exhibit varying sediment textures and slopes, which significantly influence water retention in the soil. Therefore, geomorphological data from the official cartography of PATRICOVA were used as input data. PRATICOVA categorizes different geomorphological units, including pediments, alluvial fans, splay deposits, different floodplain forms, and two types of ephemeral streams (cultivated flat-bottomed, non-cultivated V shape) (Segura-Beltrán et al., 2016).

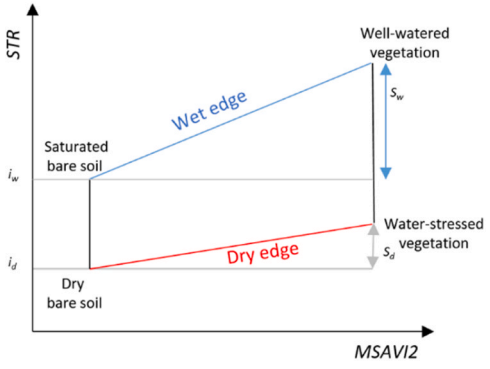

Fig. 4. Scheme illustrating the parameters of the Optical TRapezoid Model [Eqs. (3 and 4) within the space STR-MSAVI2. Adapted from Babaeian et al. (2018).

3.4. Crop data field

Crop data, such as the type of growing systems (vase and trellis) where the vines are planted, condition the canopy density and water use (Fig. 5). Bush vines are the most traditional and oldest form of vine planting. In this system, the vines grow freely without any supporting structures, creating a denser canopy that helps reduce water loss through evaporation by providing more shade to the soil and conserving moisture. This system can survive without irrigation. The trellis system involves training the vines to grow on a structure. Generally, the trellis system is beneficial for irrigation, as it allows for more efficient water distribution and helps prevent water stress in the vines. During the summer irrigation season, the grass between the rows disappears, allowing for accurate soil moisture analysis without interference from weeds. The prevailing irrigation technique in this area is drip irrigation, where the emitter wets a small portion of the surface. Information related to the specific irrigation systems used in the study area was obtained from a local information system (CRDO) connected to a vineyard layer derived from SIGPAC.

A simple random sampling method was used to train the classification between irrigated and non-irrigated plots. This method involved conducting on-site visits to fields throughout the Requena-Utiel aquifer.

The area was surveyed over several days to document the actual land conditions. The sampling involved assessing whether each plot was irrigated or rainfed. Specialized field work software, QFIELD 3.0 (QGIS Development Team, 2023) was used for data collection. This mobile app is designed for field data collection. The sampled plots ranged from a minimum area of 18 m^2 to a maximum of approximately 16 ha, ensuring they are representative of the entire area and considering the image resolution. Fig. 5 shows a map of the sampled plots at the aquifer scale. On the right side, we observe a) a plot classified as irrigated, where the drip line is located under the plant in trellis, and b) a plot classified as rainfed, with bush vines. Both aerial views illustrate the differences in plant coverage across different planting systems.

The collected data were used to train the classifier model for evaluating and assessing the accuracy of the irrigation coverage maps. Of the 686 fields visited and validated, 374 were irrigated and 212 were rainfed.

3.5. Random forest classifier

The random forest (RF) algorithm was used to build a classifier model to estimate the moisture status of the plot and assign the labels irrigated and non-irrigated. RF is a classifier with high potential for agricultural crop type classification and crop yield prediction (Devkota et al., 2024; Htitiou et al., 2019), and is superior in accuracy compared to other existing algorithms (Belgiu and Drăgu, 2016; Breiman, and Cutler, 2005). RF is a set of machine learning algorithms consisting of many decision tree classifiers, called estimators, where each tree produces its own predictions. The accuracy of the RF classifier depends on the strength of the individual tree classifiers and their dependency on each other. The forest uses averages to control overfitting (Breiman, 2001). Its architecture allows it to handle large data sets, allowing it to analyze ground, crop, and remotely sensed variables.

The estimation variables and values used in the random forest classification included a combination of qualitative and quantitative features. The specific variables used for classification were:

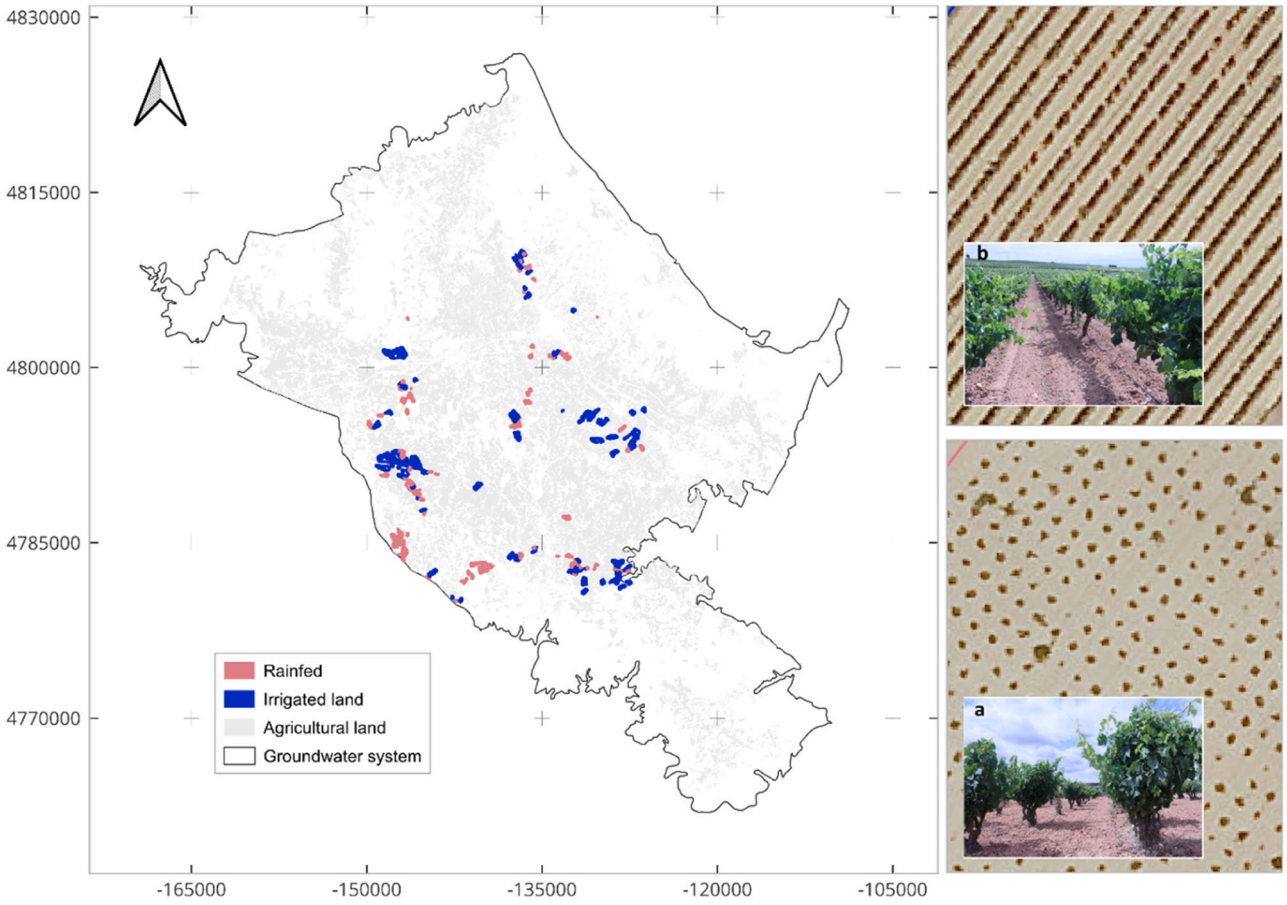

Fig. 5. The sampling map with labels assigned at the aquifer scale. On the right side, (a) illustrates a rainfed plot in bush vine, (b) represents a plot classified as irrigated, where the drip line is positioned under the plants in trellis, while. *Source of base map: Digital **aerial** orthophotographs of the Spanish **National** Orthophoto Program (**PNOA**).*

3.5.1. Qualitative Estimators (Categorical Variables)

System: Type of plantation system for the crop, such as bush and trellis. This feature helps canopy density, which impacts soil moisture.

Landforms: Geomorphological data including pediments, alluvial fans, splay deposits, floodplain forms, and ephemeral streams, which influence soil moisture retention.

3.5.2. Quantitative Estimators (Numerical Variables)

Terrain surface: Topographic data, slope and aspect, which determine the amount of solar radiation received by the soil, directly influencing soil moisture retention.

Soil Moisture Content: Estimations of soil moisture during the irrigation period, serving as a crucial indicator of crop water status.

Rainfall: Amount of rainfall during the irrigation period, which helps distinguish soil moisture due to environmental conditions from that due to irrigation input.

The combination of these qualitative and quantitative variables enables the random forest classifier to accurately classify plots as irrigated or non-irrigated plot. The algorithm takes advantage of the individual strengths of the decision tree estimators to create an ensemble model that can handle large datasets and effectively analyze spatial and agricultural variables.

Ten decision tree estimators were employed to classify the irrigated area. Two parameters were used to maximize the accuracy of the RF model: the number of predictors in each node division of the decision tree (Mtry), and the number of decision trees to run (n). Although some authors recommend setting the number of decision trees to 500, our model gave high accuracy with nTree=150. For the number of predictors in each split, Mtry = 4 was utilized, derived from the square root of the number of input variables, as recommended by researchers (Belgiu and Drăgu, 2016).

3.5.3. Accuracy assessment of classification

The dataset was split into subsets for training and validation purposes. The Random Forest (RF) model was trained and evaluated on these subsets to assess its performance. Specifically, 75 % of the dataset (510 plots) was allocated for training, while the remaining 25 % (171 plots) was set aside for testing. This approach allowed for an estimation of the model's accuracy and helped prevent issues, such as overfitting or underfitting. Additionally, a cross validation method was employed to further assess the model's performance, ensuring its ability to generalize beyond the training dataset.

A confusion matrix is provided to visualize and summarize the performance of the RF classifier (Congalton, 1991). True Positives (TP) represent cases where the model accurately predicts irrigated plots as positive. False Positives (FP) indicate cases where the model incorrectly predicts non-irrigated plots as irrigated. False Negatives (FN) denote cases where the model incorrectly predicts irrigated plot as non-irrigate. True Negatives (TN) represent cases where the model accurately predicts non-irrigated plots as negative.

Another important metric to assess the performance of machine learning models is the F1 score, which is widely used for classification tasks, particularly in scenarios with uneven class distribution. The F1 score combines two essential metrics: precision and recall. Precision quantifies the proportion of correct 'positive' predictions made by the model, while recall measures the proportion of positive class samples that the model correctly identifies.

Furthermore, predictor importance was utilized to assess the behavior of the model. This measure considers interactions with other predictors and reflects the increase in model error or decrease in accuracy when specific predictor information is removed (Molar, 2018). The importance of variables in RF classifier was determined using impurity based measures. A higher value indicates greater importance for the variable. Variable importance is computed as the normalized total of the criterion the variable contributes.

4. Results

4.1. OPTRAM-parameters

The parameterization process involved establishing a relationship between these spectral indices and soil moisture values (Fig. 6).

To perform the parametrization, the satellite images were masked to select only the pixels corresponding to vineyard land use and exclude other land uses. This ensured that the analysis focused specifically on the vineyard plot. The scatter plot of STR and MSAVI2 values for these vineyards pixels formed a cloud of points.

The lines drawn between the wet and dry points in the scatter plot created a trapezoidal shape, representing the relationship between the STR and MSAVI2 values and soil moisture. Through analysis of this trapezoidal shape, the OPTRAM model can estimate soil moisture for each pixel in the vineyard plots based on its STR and MSAVI2 values.

Interestingly, the representation of the pixel distribution during the dry season exhibited a consistent pattern across all the dates analyzed. This finding supports the hypothesis that a universal parameterization between STR, MSAVI2, and soil moisture remains relatively stable during the dry months. Consequently, the OPTRAM model can provide accurate soil moisture estimates for the vineyard plots throughout this period, (Sadeghi et al., 2017a).

The coefficients of the OPTRAM model were derived by analyzing the scatter plot depicting the relationship between the wet edge and the dry edge. The wet edge represents points corresponding to conditions where the soil has water content and the vegetation is well hydrated. Conversely, the dry edge represents points indicating conditions with lower soil moisture content and potential water stress for vegetation.

During the visual interpretation process, points that were likely affected by oversaturated or shaded pixels were omitted to ensure the accuracy and reliability of the coefficients. Oversaturated pixels occur when the sensor's sensitivity is exceeded, resulting in inaccurate measurements, while shaded pixels can produce misleading results due to reduced sunlight exposure.

In the scatter plot, the STR values serve as indicators of the amount of water content in the plant's root zone, (Babaeian et al., 2018). High STR values are typically associated with full canopy vegetation and indicate higher water content in the soil. As the vegetative vigor of the plant increases, the STR values tend to rise, indicating healthier and well-hydrated vegetation, (Sadeghi et al., 2017a).

By analyzing the scatter plot and considering the relationship between STR values, soil moisture, and vegetative vigor, the coefficients were derived to parameterize the OPTRAM model. These coefficients enable the model to estimate soil moisture based on the STR and MSAVI2 values obtained from the satellite images. The process of obtaining coefficients through visual interpretation helps ensure that the model captures the true relationship between the spectral indices and soil moisture, thereby providing accurate and meaningful estimates for soil moisture in vineyard plots.

4.2. Soil moisture mapping using OPTRAM

Soil moisture estimates exhibited different values during the irrigation period, with the lowest values obtained in July, coinciding with the low precipitation values and high temperature in the area, as reported by the station (see Fig. 2). Moisture values in some of the selected plots increased in August, also coinciding with low rainfall and high temperatures during this dry period. These higher moisture values may indicate an irrigation supply scenario in the observed plots, especially when compared with other plots experiencing minimum moisture values under similar conditions. Fig. 7 visually represents these soil moisture values over time, with the lowest values observed in July and some plots showing increased moisture in August, suggesting a potential irrigation supply scenario for those plots.

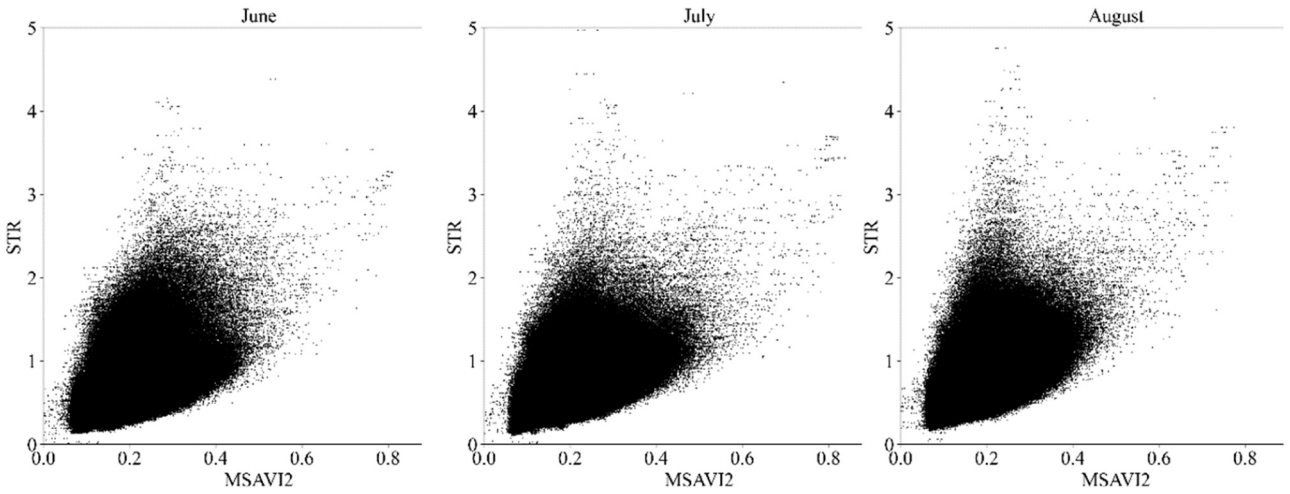

Fig. 6. Pixel distribution within the STR-MSAVI2 feature space of vineyard crop at the Requena-Utiel Aquifer during the dry period of the irrigation season of 2021.

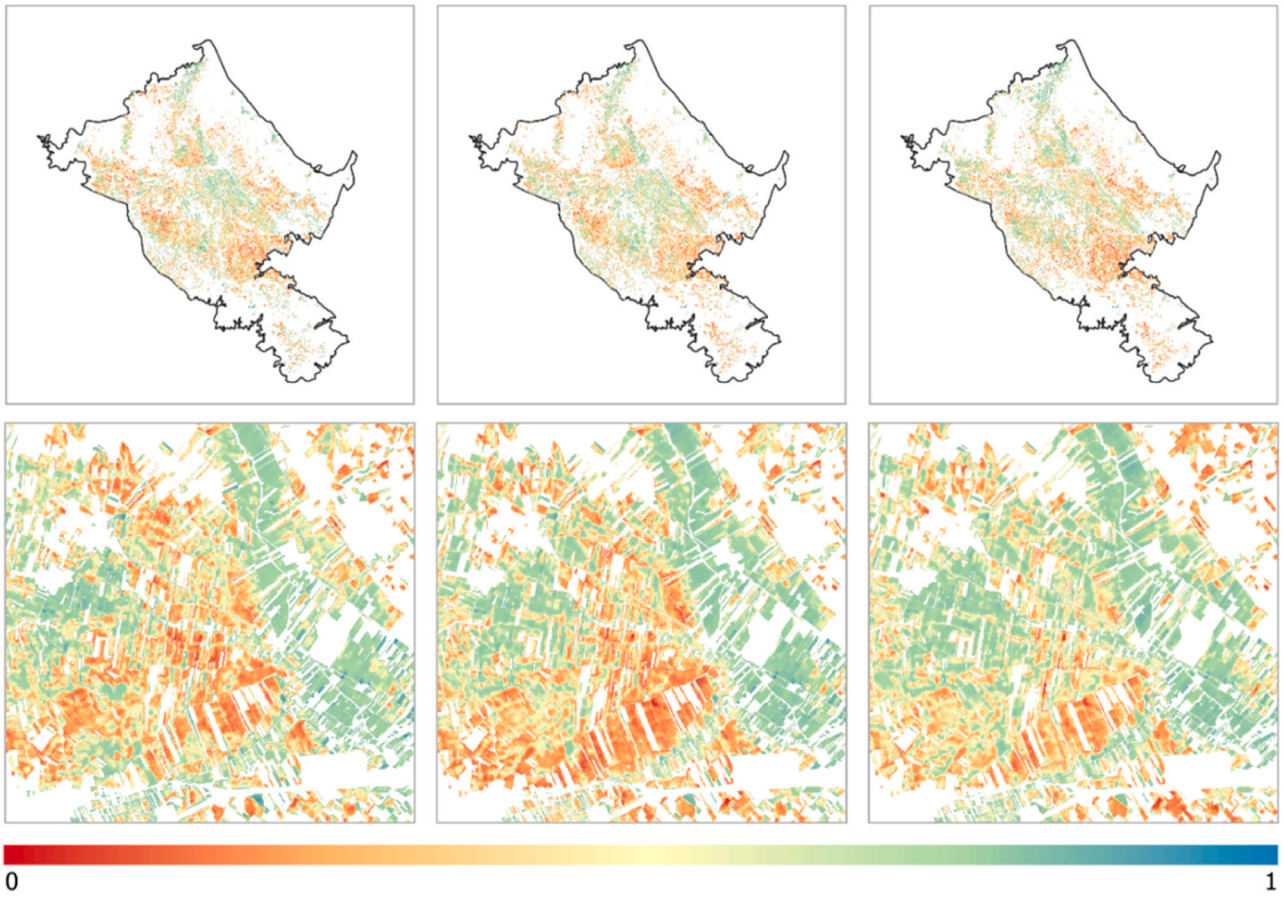

Fig. 7. Soil moisture maps generated with OPTRAM model in vineyard crop of Requena-Utiel aquifer in the dry season (June-August) of 2021. The scale ranges from 0 indicating the minimum soil moisture value, to the maximum soil moisture value.

4.3. Classification of irrigation surface

4.3.1. Variables importance

Our analysis of the importance of predictors in classifying plots as irrigated or non-irrigated during the dry season using a machine learning model is shown in Fig. 8. Notably, the predictor with the highest importance was the aspect (As), resulting in an increase in the model's error of 0.23. The moisture content of the plot varied significantly based on different orientations, with north-facing slopes showing higher soil moisture content due to reduced evaporation rates and extended moisture retention periods.

Additionally, the relationship between landforms and soil moisture is complex, influenced by various factors such as climate, geology, vegetation cover, and human activities. Specifically, landforms demonstrated lower importance in predicting the plot's status, with LD10 (Pediments) exhibiting a higher error increase compared to other landform predictors. This difference may be attributed to the properties of the pediments affecting soil moisture through changes in soil porosity,

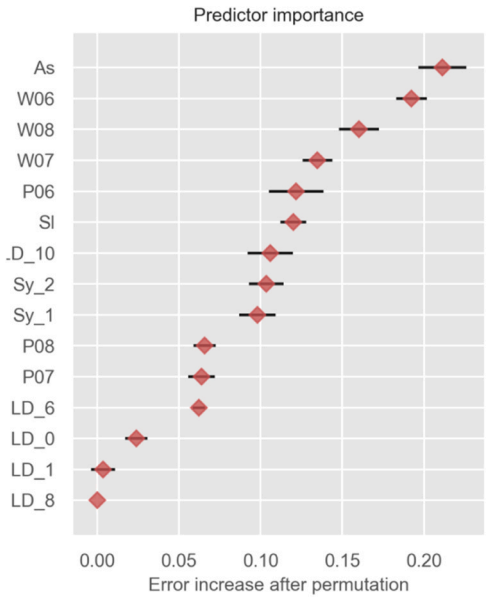

Fig. 8. Importance of each predictor for estimating the irrigated and non-irrigated area with a random forest classifier during dry season.

resulting in greater moisture-holding capacity.

Our findings highlight the significance of plot aspect, soil moisture content, and precipitation levels as crucial predictors for accurately estimating irrigated and non-irrigated areas during the dry season. In contrast, topographic features such as slope showed relatively lower importance. Understanding the relative importance of these predictors can enhance our ability to effectively manage water resources and agricultural practices during critical periods of water scarcity.

4.3.2. *Classification results*

The evaluation of accuracy was conducted by applying established approaches for identifying terrain characteristics. Table 5 displays this matrix, with the reference data (indicating irrigated and irrigated plots) represented in the columns, while the estimated outcomes obtained through machine learning techniques are depicted in the rows.

Out of the 95 plots that were actually irrigated, the model accurately identified 90 of them as irrigated, resulting in a rate of 94.74 %. However, there were 5 irrigated plots that were mistakenly classified as non-irrigated resulting in a rate of 5.26 %. On the other hand, out of the 76 plots that were non irrigated the model correctly identified 67 of them as non-irrigated, indicating a negative rate of 88.16 %. However there were 9 non-irrigated plots that were incorrectly classified as irrigated, leading to a false positive rate of 11.84 %.

The confusion matrix provides an overview of how the model performs in distinguishing between irrigated and non-irrigated plots. Although the overall accuracy, which is 91.81 % is quite high, it's important to consider the balance between true positives and false negatives, especially when it comes to managing water resources and agricultural practices. The model's ability to correctly identify non irrigated plots is commendable, but there's room for improvement in reducing misclassifications, particularly false negatives, to enhance decision making in water management.

The F1 score was also utilized to evaluate the classification model, combining two metrics: precision and recall scores, as shown in Table 6. F1 scores close to 1 indicate high precision and signify a well-performing model.

In conclusion, the random forest algorithm has been proven to be an asset for classifying areas as either irrigated or non-irrigated in the Requena Utiel region. Its accuracy and ability to handle data make it an effective tool. By analyzing the confusion matrix, we can gain insights into the model's strengths and weaknesses in predicting irrigation status. These insights are crucial for managing water resources and promoting sustainable agricultural practices.

4.4. *Irrigated area mapping*

The estimated values obtained from the machine learning classifier have facilitated the creation of surface estimations for the irrigated surface in vineyard located in the Requena-Utiel aquifer (see Fig. 9). The map distinguishes irrigated zones in blue and non-irrigated zones in

Table 2
Estimation variables and values used in the classification of random forests.

QUALITATIVE		QUANTITATIVE		
LANDFORMS (LD)	(LD2) Ephemeral streams (LD4) River Corridor (LD6) Alluvial plain (LD7) Torrential fans (LD08) Splay deposit (LD10) Pediments	TERRAIN SURFACE	Slope Aspect	(As, degrees) (Sl, m)
SYSTEMS (Sy)	(Sy1) Vase (Sy2) Trellis	PRECIPITATION (P)	June July August	P06 (mm) P07(mm) P08(mm)
		SOIL MOISTURE (W)	June July August	W06 (mm) W07 (mm) W08 (mm)

Table3
Structure of the confusion matrix.

		0	1
Actuals	0	TN	FP
	1	FN	TP
	Prediction		

Table4
The dry and wet parameters (Eq. 5) were obtained for the watershed based on S2 data for vineyard in the Requena-Utiel aquifer.

Dry edge		Wet edge	
i_d	s_d	i_w	s_w
0.00	0.40	1.2	1.5

Table 5
Confusion matrix between the predicted label and true label plots represented in percentage (number) for each row.

		Predicted label	
		Non-irr.	*Irri.*
True label	*Non-irrigated.*	67 (88.15)	9 (11.8)
	Irrigated	5 (5.3)	90 (94.7)

Table 6
F1 score and its associated metrics,.

	precision	**recall**	**F1-score**
Non-irrigated	0.93	0.88	0.91
Irrigated	0.91	0.95	0.93

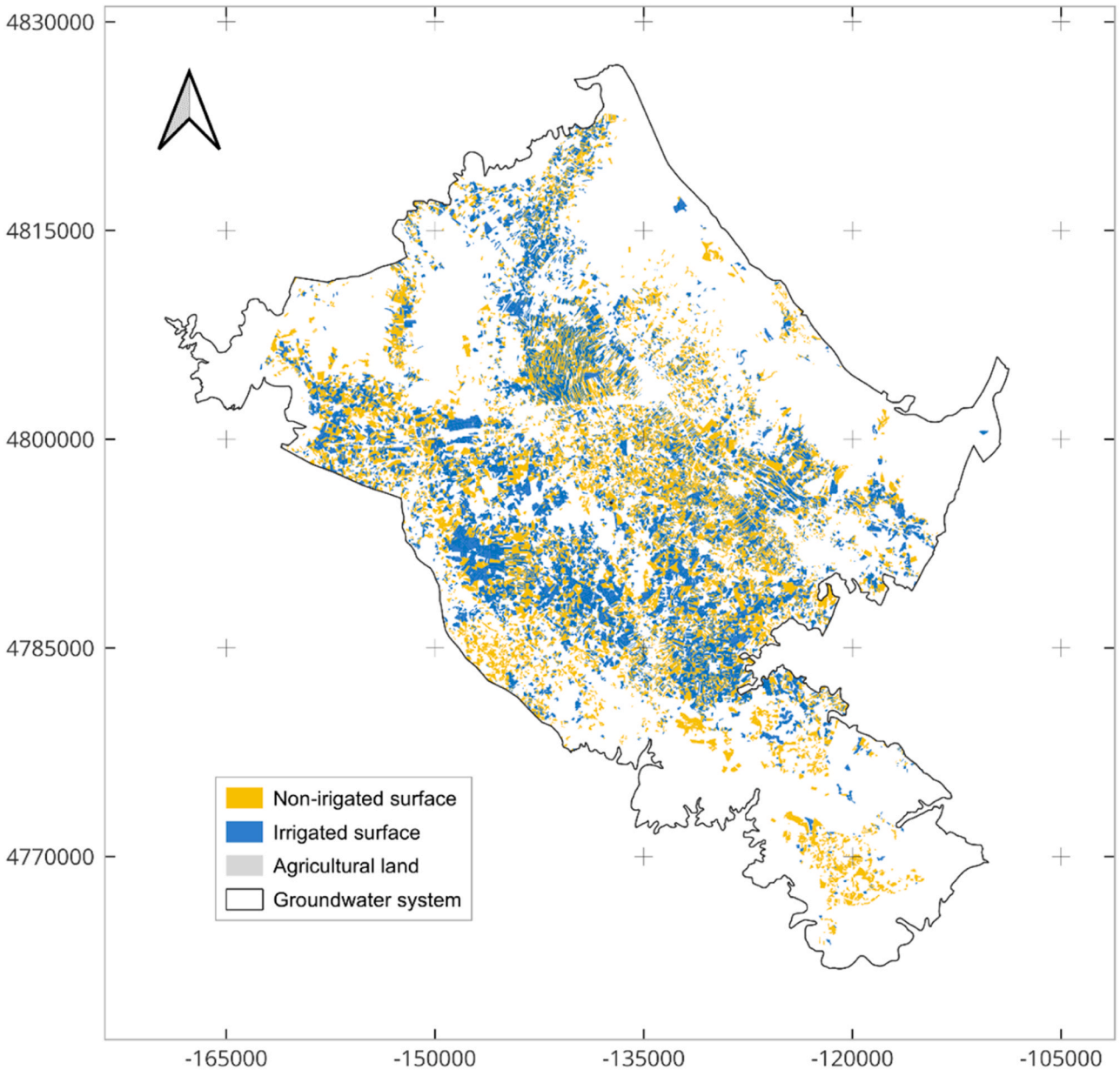

Fig. 9. Surface estimations of the irrigated (blue) and non-irrigated (yelow) surfaces in a vineyard area over theRequena-Utiel Aquifer during the irrigation season 2021.

orange. The application of classifiers to determine the water conditions of the plants has demonstrated a high level of accuracy in identifying irrigated crops. The results align with observed trends of irrigation expansion in this aquifer (Sanchis-Ibor et al., 2023), and they also exhibit logical discrepancies with statistical data.

The machine learning techniques for image classification developed in this research have detected 13,568 ha of irrigated vineyards. The error for the agricultural land cover of the Requena Utiel aquifer is 0.09. In Fig. 10, the probability of correctly labeling each class is plotted. Non irrigated areas have higher probability of being classified as false positives compared to irrigated plots.

Comparing these results with the official data on the irrigated area, the estimated values differ by 8.8 %. This difference can be considered acceptable, given the time elapsed since 2018, the fact that the River Basin Authority records rights and not actual usage, and the time lag that often occurs between the start of irrigation and the consolidation of these rights. On the other hand, the irrigated area reported by the regional government (8339 ha) is smaller than the water rights allocated by the River Basin Authority, resulting in a larger difference of 38.34 % between the regional government's survey-based data and the remote sensing detection. This discrepancy highlights an official

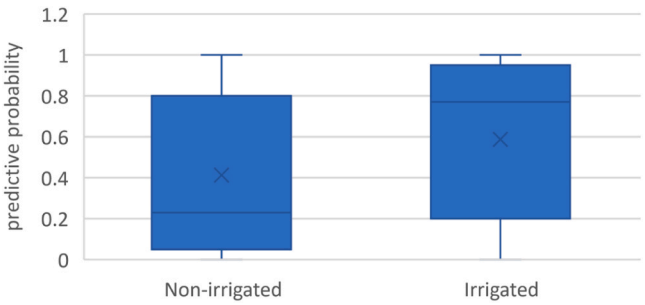

Fig. 10. The predicted probability for classificated areas.

underestimation of the irrigated area, as demonstrated by previous studies based on direct field surveys (CVER, 2007).

The applied machine learning model demonstrated that, among the data used, the aspect and soil moisture levels during the irrigation period were the most significant predictive variables. Extracted from satellites images, these variables establish the model as a reproducible method applicable to various regions. Furthermore, the comparisons made in this research highlight the effectiveness of integrating remote sensing and machine learning data to obtain an updated inventory of irrigated areas. This integration improves upon the current official records and can serve as a useful tool for monitoring irrigation expansion not only in our study area but also in similar irrigated vineyard regions. The high accuracy demonstrated by this approach establishes it as valuable assess for enhancing water resource management and optimizing agricultural planning strategies in the Requena-Utiel aquifer region. Taking advantage of the knowledge derived from our study, stakeholders can make informed decisions to ensure sustainable water usage and promote agricultural productivity in the area.

5. Discussion

The study has demonstrated the high potential of using remote sensing and artificial intelligence to estimate the irrigated area in viticultural zones, making it a valuable technique for decision-making in water planning and management. Accurately determining soil moisture content and precipitation with high and temporal resolutions is crucial for good classification results in irrigated and not irrigated vineyards. Although aspect is a limiting factor in retaining soil moisture due to the radiation it receives, it is possible that the significance of this variable would be different according to the terrain's roughness.

The integration of machine learning with remote sensing at to plot scale provides a reliable methodology for detecting and controlling irrigation expansion. By combining geographical data of water rights and obtained irrigation plots, it becomes possible to identify presumably irrigated lands without proper rights. Considering the margin of error of this methodology, it can considerably facilitate inspection works in a cost-effective manner. Moreover, the use of these technological tools based on remote sensing, highly valued by local irrigators (Sanchis-Ibor et al., 2023) has a deterrent effect on free-riders, as demonstrated in other areas (Calera et al., 2017; Rouillard et al., 2021).

Despite the good fit of the model results, the approach has certain limitations in practical application. Firstly, the baseline data obtained through random sampling may be improved by using a cluster sampling approach, which can save costs and simplify data collection (Stehman, 2009; Stehman and Foody, 2019). Secondly, the model error used in machine learning techniques assesses accuracy on the available dataset and may yield larger errors when predictions are made outside the range of the training data. Thirdly, the OPTRAM method's ability to estimate soil moisture can be hindered by oversaturated and shaded pixels (Sadeghi et al., 2017b). These limitations should be considered when applying the methodology in practical scenarios. Finally, it is important to consider research that highlights the cautious approach required when using ML techniques for knowledge discovery in digital soil mapping. This is due to the limitations of drawing causal conclusions from variable importance measures, (Wadoux et al., 2020).

Additionally, the lack of an up-to-date database of irrigated areas poses challenges in training artificial intelligence algorithms. Therefore, the methodology relies on extensive fieldwork, which may gradually reduce as more real field data becomes available. It is essential to continue collecting data to refine the models and improve their accuracy. This iterative process will contribute to enhancing the reliability and effectiveness of the methodology over time.

In the future, further research in this area should focus on obtaining a longer time series of OPTRAM parameters and refining machine learning models to adapt to changing environmental conditions. With these advancements, the integration of remote sensing and artificial intelligence will undoubtedly play a pivotal role in shaping sustainable water management strategies. This will enable a enabling a more precise and up-to-date inventory of irrigated areas, and contributing to the conservation of precious water resources in agricultural regions worldwide. This forward-thinking approach holds promise for addressing the challenges of water scarcity and promoting more efficient agricultural practices in line of evolving environmental conditions.

CRediT authorship contribution statement

Esther Lopez-Perez: Conceptualization, Data curation, Formal analysis, Investigation, Methodology, Software, Validation, Visualization, Writing – original draft, Writing – review & editing. **Manuel Pulido Velazquez:** Funding acquisition, Investigation, Project administration, Supervision, Writing – review & editing. **Miguel Angel Jiménez-Bello:** Formal analysis, Investigation, Methodology, Software, Supervision, Validation, Writing – original draft, Writing – review & editing. **Carles Sanchis-Ibor:** Conceptualization, Formal analysis, Investigation, Methodology, Supervision, Validation, Writing – original draft, Writing – review & editing.

Declaration of Competing Interest

The authors declare that they have no known competing financial interests or personal relationships that could have appeared to influence the work reported in this paper

Data availability

Data will be made available on request.

Acknowledgments

This work was funded by the eGROUNDWATER Project (GAn.1921) as part of the PRIMA programme supported by the European Union's Horizon2020 Research and Innovation Programme. We thank Utiel-Requena Designation of Origin for providing crop information. We also thank two anonymous reviewers for the constructive comments that greatly improved the manuscript.

References

Akbari, E., Boloorani, A.D., Samany, N.N., Hamzeh, S., Soufizadeh, S., Pignatti, S., 2020. Crop mapping using random forest and particle swarm optimization based on multi-temporal sentinel-2. Remote Sens. 12, 1–21. https://doi.org/10.3390/RS12091449.

Ambika, A.K., Wardlow, B., Mishra, V., 2016. Remotely sensed high resolution irrigated area mapping in India for 2000 to 2015. Sci. Data 3, 1–14. https://doi.org/10.1038/sdata.2016.118.

Ameur, F., Amichi, H., Kuper, M., Hammani, A., 2017. Specifying the differentiated contribution of farmers to groundwater depletion in two irrigated areas in North Africa. Hydrogeol. J. 25 (6), 1579–1591. https://doi.org/10.1007/s10040-017-1569-1.

Babaeian, E., Sadeghi, M., Franz, T.E., Jones, S., Tuller, M., 2018. Mapping soil moisture with the OPtical TRApezoid Model (OPTRAM) based on long-term MODIS observations. Remote Sens. Environ. 211, 425–440. https://doi.org/10.1016/j.rse.2018.04.029.

Babaeian, E., Sidike, P., Newcomb, M.S., Maimaitijiang, M., White, S.A., Demieville, J., Ward, R.W., Sadeghi, M., LeBauer, D.S., Jones, S.B., Sagan, V., Tuller, M., 2019. A new optical remote sensing technique for high-resolution mapping of soil moisture. Front. Big Data 2, 1–6. https://doi.org/10.3389/fdata.2019.00037.

Ballester-Berman, J.D., Vicente-Guijalba, F., Lopez-Sanchez, J.M., 2013. Polarimetric sar model for soil moisture estimation over vineyards at C-band. Prog. Electromagn. Res. 142, 639–665. https://doi.org/10.2528/PIER13071702.

Bazzi, H., Baghdadi, N., Ienco, D., Hajj, M., El, Zribi, M., Belhouchette, H., Escorihuela, M.J., Demarez, V., 2019. Mapping irrigated areas using Sentinel-1 time series in Catalonia, Spain. Remote Sens. 11, 1–25. https://doi.org/10.3390/rs11151836.

Belgiu, M., Drăgu, L., 2016. Random forest in remote sensing: A review of applications and future directions. ISPRS J. Photogramm. Remote Sens. 114, 24–31. https://doi.org/10.1016/j.isprsjprs.2016.01.011.

Birkenholtz, T.L., 2015. Recentralizing groundwater governmentality: rendering groundwater and its users visible and governable. WIREs Water 2, 21–30. https://doi.org/10.1002/wat2.1058.

Blaschke, T., 2010. Object based image analysis for remote sensing. ISPRS J. Photogramm. Remote Sens. 65, 2–16. https://doi.org/10.1016/j.isprsjprs.2009.06.004.

Bouasria, A., Rahimi, A., Mjiri, I.El, Namr, K.I., Ettachfini, E.M., Bounif, M., 2021b. Comparative study between two methods of crop classification in the irrigated area of Sidi Bennour, 2021 3rd Int. Sustain. Resil. Conf. Clim. Chang 500–503. https://doi.org/10.1109/IEEECONF53624.2021.9668069.

Bouasria, A., Rahimi, A., El Mjiri, I., Namr, K.I., Ettachfini, E.M., Bounif, M., 2021a. Use of remote sensing data to estimate sugar beet crop yield in the Doukkala Irrigated Perimeter, 2021 3rd Int. Sustain. Resil. Conf. Clim. Chang 504–507. https://doi.org/10.1109/IEEECONF53624.2021.9668059.

Bounif, M., Bouasria, A., Rahimi, A., El Mjiri, I., 2021. Study of agricultural land use variability in Doukkala irrigated area between 1998 and 2020. 2021 3rd Int. Sustain. Resil. Conf. Clim. Chang 170–175. https://doi.org/10.1109/IEEECONF53624.2021.9667965.

Breiman, Cutler, A., 2005. Random forests [WWW Document]. Random. https://doi.org/10.4324/9781003109396-5.

Breiman, L., 2001. Random forests. Random 1–122. https://doi.org/10.1201/9780429469275-8.

Brodley, C.E., Friedl, M.A., 1997. Decision tree classification of land cover from remotely sensed data. Remote Sens. Environ. 61, 399–409. https://doi.org/10.1016/S0034-4257(97)00049-7.

Brown, J.F., Pervez, M.S., 2014. Merging remote sensing data and national agricultural statistics to model change in irrigated agriculture. Agric. Syst. 127, 28–40. https://doi.org/10.1016/j.agsy.2014.01.004.

Calera, A., Garrido-Rubio, J., Belmonte, M., Arellano, I., Fraile, L., Campos, I., Osann, A., 2017. Remote sensing-based water accounting to support governance for groundwater management for irrigation in la Mancha oriental aquifer, Spain. WIT Trans. Ecol. Environ. 220, 119–126. https://doi.org/10.2495/WRM170121.

Castaño, S., Sanz, D., Gómez-Alday, J.J., 2010. Methodology for quantifying groundwater abstractions for agriculture via remote sensing and GIS. Water Resour. Manag. 24, 795–814. https://doi.org/10.1007/s11269-009-9473-7.

Chen, M., Zhang, Y., Yao, Y., Lu, J., Pu, X., Hu, T., Wang, P., 2020. Evaluation of the OPTRAM model to retrieve soil moisture in the Sanjiang Plain of Northeast China. Earth Sp. Sci. 7 https://doi.org/10.1029/2020EA001108.

CHJ (2016) the Exploitation plan of the Requena-Utiel groundwater body. Confederación Hidrográfica del Júcar, Available online: https://www.chj.es/es-es/medioambiente/PlanExplotacion.

CHJ (2019) Registro de concesiones de aguas. Comisaría de Aguas. Confederación Hidrográfica del Júcar.

CHJ (2020) Review exploitation plan of the Requena-Utiel groundwater body. Confederación Hidrográfica del Júcar, Available online: https://www.chj.es/es-es/medioambiente/PlanExplotacion.

Closas, A., Molle, F., Hernández-Mora, N., 2017. Sticks and carrots to manage groundwater over-abstraction in La Mancha, Spain. Agric. Water Manag. 194, 113–124. https://doi.org/10.1016/j.agwat.2017.08.024.

Congalton, R.G., 1991. A review of assessing the accuracy of classifications of remotely sensed data. Remote Sens. Environ. 37, 35–46. https://doi.org/10.1016/0034-4257(91)90048-B.

CVER (2007). Estudio de las necesidades hídricas de la comarca del Vinalopó Medio en la demarcación hidrográfica del Júcar. Report. Centro Valenciano de Estudios del Riego - Confederación Hidrográfica del Júcar.

Damonte, D., Boelens, R., 2019. Hydrosocial territories, agro-export and water scarcity: capitalist territorial transformations and water governance in Peru's coastal valleys. Water Int. 44 (2), 206–223. https://doi.org/10.1080/02508060.2018.1556869.

Dari, J., Quintana-Seguí, P., Escorihuela, M.J., Stefan, V., Brocca, L., Morbidelli, R., 2021. Detecting and mapping irrigated areas in a Mediterranean environment by using remote sensing soil moisture and a land surface model. J. Hydrol. 596 https://doi.org/10.1016/j.jhydrol.2021.126129.

De Stefano, L., López-Gunn, E., Martínez-Santos, P., 2014. Intensive groundwater use in agriculture and IWRM: An impossible marriage? In: Martinez-Santos, P., Aldaya, M. M., Llamas, M.R. (Eds.), Integrated water resources management in the 21st century: Revisiting the paradigm. CRC Press, Leiden, The Netherlands.

De Stefano, L., Fornés, J.M., López-Geta, J.A., Villarroya, F., 2015. Groundwater use in Spain: an overview in light of the EU Water Framework Directive. Int. J. Water Resour. Dev. 31 (4), 640–656. https://doi.org/10.1080/07900627.2014.938260.

Devkota, K.P., Bouasria, A., Devkota, M., Nangia, V., 2024. Predicting wheat yield gap and its determinants combining remote sensing, machine learning, and survey approaches in rainfed Mediterranean regions of Morocco. Eur. J. Agron. 158, 127195 https://doi.org/10.1016/j.eja.2024.127195.

Foster, T., Mieno, T., Brozović, N., 2020. Satellite-based monitoring of irrigation water use: assessing measurement errors and their implications for agricultural water management policy. Water Resour. Res. 56 https://doi.org/10.1029/2020WR028378.

Funk, C., Peterson, P., Landsfeld, M., Pedreros, D., Verdin, J., Shukla, S., Husak, G., Rowland, J., Harrison, L., Hoell, A., Michaelsen, J., 2015. The climate hazards infrared precipitation with stations - a new environmental record for monitoring extremes. Sci. Data 2. https://doi.org/10.1038/sdata.2015.66.

Gao, Q., Zribi, M., Escorihuela, M.J., Baghdadi, N., 2017. Synergetic use of sentinel-1 and sentinel-2 data for soil moisture mapping at 100m resolution. Sens. (Switz.) 17. https://doi.org/10.3390/s17091966.

Gao, Q., Zribi, M., Escorihuela, M.J., Baghdadi, N., Segui, P.Q., 2018. Irrigation mapping using Sentinel-1 time series at field scale. Remote Sens. 10 https://doi.org/10.3390/rs10091495.

Giordano, M., 2009. Global groundwater? Issues and solutions. Annu. Rev. Environ. Resour. 34, 153–178. https://doi.org/10.1146/annurev.environ.030308.100251.

Gleeson, T., Wada, Y., Bierkens, M.F.P., Van Beek, L.P.H., 2012. Water balance of global aquifers revealed by groundwater footprint. Nature 488, 197–200. https://doi.org/10.1038/nature11295.

Grogan, D.S., Wisser, D., Prusevich, A., Lammers, R.B., Frolking, S., 2017. The use and re-use of unsustainable groundwater for irrigation: a global budget. Environ. Res. Lett. 12 https://doi.org/10.1088/1748-9326/aa5fb2.

GVA 2021. Estadística sobre superficies y producciones anuales de cultivo, Generalitat Valencia,Conselleria de Agricultura, Desarrollo Rural, Emergencia Climática y Transición Ecológica.

Hoogesteger, J., Wester, P., 2015. Intensive groundwater use and (in)equity: Processes and governance challenges. Environ. Sci. Policy. https://doi.org/10.1016/j.envsci.2015.04.004.

Hoogesteger, J., Wester, P., 2018. Gestión del agua subterránea de uso agrícola: los retos de la sustentabilidad socio-ambiental y la equidad. Cuad. Geogr. la Univ. Val. ència 51. https://doi.org/10.7203/cguv.101.13720.

Htitiou, A., Boudhar, A., Lebrini, Y., Hadria, R., Lionboui, H., Elmansouri, L., Tychon, B., Benabdelouahab, T., 2019. The performance of random forest classification based on phenological metrics derived from sentinel-2 and Landsat 8 to map crop cover in an irrigated semi-arid region. Remote Sens. Earth Syst. Sci. 2, 208–224. https://doi.org/10.1007/s41976-019-00023-9.

Llamas, M.R., Martínez-Santos, P., 2005. Intensive groundwater use: silent revolution and potential source of social conflicts. J. Water Resour. Plan. Manag. 131, 337–341. https://doi.org/10.1061/(asce)0733-9496(2005)131:5(337).

López-Gunn, E., 2012. Groundwater governance and social capital. Geoforum 43, 1140–1151. https://doi.org/10.1016/j.geoforum.2012.06.013.

Mananze, S., Pôças, I., 2019. Agricultural drought monitoring based on soil moisture derived from the optical trapezoid model in Mozambique. J. Appl. Remote Sens. 13, 1. https://doi.org/10.1117/1.jrs.13.024519.

Mjiri, I.El, Rahimi, A., Bouasria, A., Bounif, M., 2022. Using RapidEye satellite images for the sustainable management of the extension of El Jadida city (Morocco), 2022 Int. Conf. Decis. Aid Sci. Appl. DASA 2022, 761–765. https://doi.org/10.1109/DASA54658.2022.9765099.

Molar, C. 2018. Interpretable Machine Learning. Retrieved from https://christophm.github.io/interpretable-ML-book/.

Molle, F., Closas, A., 2020. Why is state-centered groundwater governance largely ineffective? A review. Wiley Interdiscip. Rev. Water 7, 1–17. https://doi.org/10.1002/wat2.1395.

Molle, F., López-Gunn, E., van Steenbergen, F., 2018. The local and national politics of groundwater overexploitation. Water Alter. 11, 445–457.

Pageot, Y., Baup, F., Inglada, J., Baghdadi, N., Demarez, V., 2020. Detection of irrigated and rainfed crops in temperate areas using sentinel-1 and sentinel-2 time series. Remote Sens 12, 1–19. https://doi.org/10.3390/RS12183044.

PATRICOVA, 2021.Pla d'acció territorial de caràcter sectorial sobre prevenció del risc d'inundació a la Comunitat Valenciana, Generalitat Valenciana. Retrieved from: https://politicaterritorial.gva.es/va/web/planificacion-territorial-e-infraestructura-verde/cartografia-del-patricova.

Qi J., Kerr Y., C.A., 1994. External_factor_consideration_in_vegetat.pdf.

Qi, J., Chehbouni, A., Huete, A.R., Kerr, Y.H., Sorooshian, S., 1994. A modified soil adjusted vegetation index. Remote Sens. Environ. 48, 119–126. https://doi.org/10.1016/0034-4257(94)90134-1.

Rabiei, S., Jalilvand, E., Tajrishy, M., 2021. A method to estimate surface soil moisture and map the irrigated cropland area using sentinel-1 and sentinel-2 data. Sustain 13. https://doi.org/10.3390/su132011355.

Rahimi, A., Bouasria, A., Bounif, M., Zaakour, F., El Mjiri, I., 2021. Estimating evapotranspiration using remote sensing and the METRIC energy balance model: Case study of Sidi Benour region (Morocco), 2021 3rd Int. Sustain. Resil. Conf. Clim. Chang 142–147. https://doi.org/10.1109/IEEECONF53624.2021.9667981.

Rahimi, A., El Mjiri, I., Bouasria, A., Zaakour, F., 2022. Applying machine learning to the study of environmental dynamics and sustainable management of the Argan grove in the El Guerdane region (Souss plain, Morocco). 2022 Int. Conf. Decis. Aid Sci. Appl. DASA 2022 766–770. https://doi.org/10.1109/DASA54658.2022.9765214.

Richardson, A.J., Wiegand, C.L., 1977. Distinguishing vegetation from soil background information. Photogramm. Eng. Remote Sens. 43, 1541–1552.

Sadeghi, M., Jones, S.B., Philpot, W.D., 2015. A linear physically-based model for remote sensing of soil moisture using short wave infrared bands. Remote Sens. Environ. 164, 66–76. https://doi.org/10.1016/j.rse.2015.04.007.

Sadeghi, M., Babaeian, E., Tuller, M., Jones, S.B., 2017a. The optical trapezoid model: A novel approach to remote sensing of soil moisture applied to Sentinel-2 and Landsat-8 observations. Remote Sens. Environ. 198, 52–68. https://doi.org/10.1016/j.rse.2017.05.041.

Sadeghi, M., Babaeian, E., Tuller, M., Jones, S.B., 2017b. The optical trapezoid model: A novel approach to remote sensing of soil moisture applied to Sentinel-2 and Landsat-8 observations. Remote Sens. Environ. 198, 52–68. https://doi.org/10.1016/j.rse.2017.05.041.

Sanchis-Ibor, C., López-Pérez, E., García-Mollá, M., López-Gunn, E., Rubio-Martín, A., Pulido-Velazquez, M., Segura-Calero, S., 2023. Advancing Co-governance through Framing Processes: Insights from Action- Research in the Requena- Utiel Aquifer (Eastern Spain). Int. J. Commons 17, 347–362. https://doi.org/10.5334/ijc.1355.

Segura-Beltrán, F., Sanchis-Ibor, C., Morales-Hernández, M., González-Sanchis, M., Bussi, G., Ortiz, E., 2016. Using post-flood surveys and geomorphologic mapping to evaluate hydrological and hydraulic models: The flash flood of the Girona River (Spain) in 2007. J. Hydrol. 541, 310–329. https://doi.org/10.1016/j.jhydrol.2016.04.039.

Shah, T., Burke, J., Villholth, K., Angelica, M., Custodio, E., Daibes, F., Hoogesteger, J., Giordano, M., Girman, J., van der Gun, J., Kendy, E., Kijne, J., Llamas, R., Masiyandama, M., Margat, J., Marin, L., Peck, J., Rozelle, S., Sharma, B., Vincent, L.,

Wang, J., 2007. Groundwater: A global assessment of scale and significance, in: Water for Food Water for Life: A Comprehensive Assessment of Water Management in Agriculture. pp. 395–424. https://doi.org/10.4324/9781849773799.
Sharma, A.K., Hubert-Moy, L., Buvaneshwari, S., Sekhar, M., Ruiz, L., Moger, H., Bandyopadhyay, S., Corgne, S., 2021. Identifying seasonal groundwater-irrigated cropland using multi-source NDVI time-series images. Remote Sens 13, 1–21. https://doi.org/10.3390/rs13101960.
Sharples, J. Carrara, E., Preece, L., Chery, L., López, B.,Rinaudo, J.-D. 2020.Information Systems for Sustainable Management of Groundwater Extraction in France and Australia In: J.D. Rinaudo et al. (eds.), Sustainable Groundwater Management, Global Issues in Water Policy 24, https://doi.org/10.1007/978-3-030-32766-8_9.
SIGPAC, 2021. Institut cartogràfic València. Available online: ⟨https://geocataleg.gva.es/#/search?uuid=spa_icv_sigpac_2021_recintos&lang=spa⟩ (accessed on 1 February 2021).
Stehman, S.V., 2009. Sampling designs for accuracy assessment of land cover. Int. J. Remote Sens. 30, 5243–5272. https://doi.org/10.1080/01431160903131000.
Stehman, S.V., Foody, G.M., 2019. Key issues in rigorous accuracy assessment of land cover products. Remote Sens. Environ. 231, 111199 https://doi.org/10.1016/j.rse.2019.05.018.
Towers, P.C., Strever, A., Poblete-Echeverría, C., 2019. Comparison of vegetation indices for leaf area index estimation in vertical shoot positioned vine canopies with and without grenbiule hail-protection netting. Remote Sens 11. https://doi.org/10.3390/rs11091073.
Vogels, M.F.A., de Jong, S.M., Sterk, G., Addink, E.A., 2019. Mapping irrigated agriculture in complex landscapes using SPOT6 imagery and object-based image analysis – A case study in the Central Rift Valley, Ethiopia. Int. J. Appl. Earth Obs. Geoinf. 75, 118–129. https://doi.org/10.1016/j.jag.2018.07.019.
Wadoux, A.M.J.C., Samuel-Rosa, A., Poggio, L., Mulder, V.L., 2020. A note on knowledge discovery and machine learning in digital soil mapping. Eur. J. Soil Sci. 71, 133–136. https://doi.org/10.1111/ejss.12909.
Wigneron, J., Jackson, T.J., Neill, P.O., Lannoy, G., De, Rosnay, P., De, Walker, J.P., Ferrazzoli, P., Mironov, V., Bircher, S., Grant, J.P., Kurum, M., Schwank, M., Das, N., Royer, A., Bitar, A., Al, Lawrence, H., Mialon, A., Parrens, M., Richaume, P., Delwart, S., Kerr, Y., 2017. Modelling the passive microwave signature from land surfaces: A review of recent results and application to the L-band SMOS & SMAP soil moisture retrieval algorithms. Remote Sens. Environ. 192, 238–262. https://doi.org/10.1016/j.rse.2017.01.024.
Wigneron, J.-P., Calvet, J.-C., Kerr, Y., 1996. Monitoring water interception by crop fields from passive microwave observations. Agric. . Meteorol. 80, 177–194. https://doi.org/10.1016/0168-1923(95)02296-1.
Xie, Y., Gibbs, H.K., Lark, T.J., 2021. Landsat-based Irrigation Dataset (LANID): 30m resolution maps of irrigation distribution, frequency, and change for the US, 1997-2017. Earth Syst. Sci. Data 13, 5689–5710. https://doi.org/10.5194/essd-13-5689-2021.
Xue, J., Su, B., 2017. Significant remote sensing vegetation indices: A review of developments and applications. J. Sens. 2017 https://doi.org/10.1155/2017/1353691.
Zohaib, M., Kim, H., Choi, M., 2019. Detecting global irrigated areas by using satellite and reanalysis products. Sci. Total Environ. 677, 679–691. https://doi.org/10.1016/j.scitotenv.2019.04.365.
Zurqani, H.A., Allen, J.S., Post, C.J., Pellett, C.A., Walker, T.C., 2021. Mapping and quantifying agricultural irrigation in heterogeneous landscapes using Google Earth Engine. Remote Sens. Appl. Soc. Environ. 23, 100590 https://doi.org/10.1016/j.rsase.2021.100590.

Further reading

Rinaudo, J.D., Donoso, G., 2019. State, market or community failure? Untangling the determinants of groundwater depletion in Copiapó (Chile). Int. J. Water Resour. Dev. 35 (2), 283–304. https://doi.org/10.1080/07900627.2017.1417116.